J. Fluid Mech. (1992), *vol.* 238, *pp.* 633–656
Printed in Great Britain

Almost symmetric solitary eddies in a two-layer ocean

By G. G. SUTYRIN[1] AND W. K. DEWAR[2]

[1] P. P. Shirshov Institute of Oceanology, USSR Academy of Sciences, Krasikova 23, 117218, Moscow, USSR

[2] Department of Oceanography, Florida State University, Tallahasee, FL 32306, USA

(Received 2 July 1991 and in revised form 15 October 1991)

An asymptotic theory of two-dimensional planetary solitary eddies is presented. Previous studies in one-and-a-half layer models have discovered special classes of radially symmetric structure which are associated with eddies of permanent form. We generalize these studies by including an active lower layer and by considering the effects of azimuthal structure. Accordingly, we stress two main results; namely, (i) permanent-form two-layer eddies with essentially arbitrary radial structure exist, provided that the eddy includes a weak imbedded dipolar asymmetry and an appropriate counter-rotating deep flow, and (ii) fluid trapped under an eddy in Taylor columns can significantly affect eddy properties if the trapped fluid possesses non-trivial potential vorticity.

The structural permanency in our solutions arises from a balance between nonlinear steepening, driven by the continuity equation, and planetary dispersion. The structural asymmetries affect eddy propagation, either by dipole interaction within the layer (as occurs in modons) or by pressure forces acting between layers. The primary role of the deep counter-rotating flow is to balance the net upper-layer transport. The interesting layer–layer interaction, however, involves higher-order dynamics and is sensitive to the continuity of the potential-vorticity field. In general, these eddies trap fluid both in the upper thermocline and in the lower layer.

The dominance of oceanic anticyclones over cyclones is relatively well known. A main conclusion of this study is that the class of long-lived anticyclones is considerably broader than previously realized. This may help explain the observed bias toward anticyclonic eddies. A second conclusion is that estimates of material transport by eddies may need to account for the movement of fluid outside the main bowl of the eddies.

1. Introduction

Much attention has been paid in recent years to naturally occurring long-lived vortices. Examples range from the Great Red Spot of Jupiter (as well as other more recently discovered planetary spots) to several types of ocean eddies. Distinguishing features of these vortices include their apparent robustness to disturbances, their dominance of their surroundings in strength and amplitude and their monopole structure. Such vortices are commonly referred to as coherent vortices, and in this paper an asymptotic theory of long-lived vortices is presented.

In the oceanographic setting, which constitutes the primary motivation for the present study, estimates suggest that the number of such long-lived vortices is overwhelming. For example, based on a recent census of anomalous water parcels,

Ebbesmeyer *et al.* (1986) argue that there may be from 1000 to 10000 such vortices present in the North Atlantic at any one time. This population density, coupled with the observation that such eddies possess and transport extreme property anomalies, suggests that coherent vortices participate importantly in the distribution of passive and dynamic tracers in the world's oceans. This class of eddies has been named 'submesoscale coherent vortices' (SCVs) and are observed to be predominantly anticyclonic (McWilliams 1985).

Another oceanographic example of long-lived vortices is those associated with western boundary currents (e.g. Gulf Stream rings, Kuroshio rings). These form at a rate of several per year and are observed to transport considerable mass across their parent current. Both stable cyclones and stable anticyclones (i.e. cold and warm core respectively) have been observed, although certain currents, like the Agulhas, mostly form anticyclones.

Although the dynamic role of coherent vortices in the world ocean has not yet been unambiguously identified, the above observations have motivated several relevant theoretical studies. This interest is partly motivated by experience in other branches of fluid mechanics, such as the study of surface gravity waves. There, it is recognized that coherent features (i.e. 'solitons') frequently arise in the evolution of a given field. A similar role has not yet been demonstrated for coherent vortices in geophysical fluid dynamics (GFD) (but see McWilliams 1984), but it remains a possibility that the predictability of ocean currents could be enhanced by the apparent propensity of the ocean to generate long-lived structures. To this end, Charney & Flierl (1981) speculate on the importance of solitary-wave behaviour in the oceans at scales larger than the deformation radius.

A unifying theme of analytical GFD vortex studies is their attention to permanent-form, steadily propagating structures, which are in turn simplifications motivated by observations. Perhaps the best known class of coherent vortices is the 'modons' (Stern 1975; see also the excellent review by Flierl 1987), which belong to the general category of dipoles. Such vortices have been studied in barotropic, reduced-gravity (Larichev & Reznik 1976), two-layer (Flierl *et al.* 1980) and continuously stratified (Berestov 1981) fluids. A distinguishing feature of modons is that their potential-vorticity function is non-analytic; that is, their potential-vorticity structure within closed streamlines differs from that on streamlines connected to the far field. The laboratory study of Flierl, Stern & Whitehead (1983) argues for the participation of modons in the evolution of rather general eddy initial-value problems. Nonetheless, the application of modons to the understanding of oceanic vortices appears to be limited, as observed eddies are dominantly radially symmetric. No convincing evidence of dipole structure in either SCVs or rings has yet been found.

It has been proposed by several authors that radially symmetric coherent vortices are described by a two-dimensional KdV equation. Flierl (1979) and Malanotte-Rizzoli (1982) discuss such solutions within the quasi-geostrophic framework. In that parameter range, the requisite steepening of KdV dynamics is driven by external sources, such as a large-scale shear flow (as in Flierl) or topography (as in Malanotte-Rizzoli). Subsequent to these studies, it was noticed almost simultaneously by Mikhailova & Shapiro (1980), Petviashvili (1980), Charney & Flierl (1981), Yamagata (1982) and Petviashvili & Yan'kov (1982) that KdV dynamics describe weakly nonlinear, solitary eddies on a beta-plane (see also Flierl 1987). The steepening in these equations is driven by the nonlinear advection of buoyancy and is thus internal to the eddies (although, interestingly, the above authors derived equations similar to that discussed by Flierl 1979). The analysis applies to either barotropic or reduced-

gravity systems (i.e. lower layer at rest), and solutions for the radial structure were provided by Charney & Flierl (1981) and Petviashvili & Yan'kov (1982). Result of these studies is that solitary, shape-preserving solutions exist for anticyclones, but not for cyclones.

Many coherent vortices have been observed to be thick relative to the environment in which they reside, i.e. the vertical scale of a given ring can be $O(800$ m) in a fluid of total depth $O(4000$ m). The ratio of these thicknesses (0.2) is thus comparable in magnitude to other small parameters describing ring dynamics. This recommends the study of rings in systems with active lower layers, as opposed to reduced-gravity systems. Two important first contributions along these lines were made by Flierl (1984*a*, *b*) who generalized an earlier reduced-gravity solution proposed by Nof (1981). Flierl argued that drifting rings generally radiate planetary waves. These, in turn, slow the westward ring migration and induce a southward ring drift. Most recent progress on rings in multi-layer systems has been numerical and has employed a variety of equations. Examples are balanced model calculations (McWilliams, Gent & Norton 1986), 'filtered' generalized geostrophic calculations (Tang & Cushman-Roisin 1992; Cushman-Roisin, Sutyrin & Tang 1992) and 'unfiltered' primitive equation calculations (Chassignet & Cushman-Roisin 1991). Many of these studies have emphasized the role of wave radiation on eddy propagation, and the relative stability of anticyclones compared to cyclones (Matsuura & Yamagata 1982; Sutyrin & Yushina 1986).

In spite of the considerable progress made on the study of coherent vortices, many interesting questions remain. For example, it is unclear how the radially symmetric solitary waves found in reduced-gravity systems respond to the presence of an active lower layer. Indeed, it is unknown if stationary-state vortex solutions in two-layer systems exist. Also, simple scaling arguments suggest that regions of trapped fluid will develop under oceanic eddies, in a manner reminiscent of Taylor columns trapped over bottom obstacles. A classical question in eddy dynamics pertains to the effects of such trapped fluid (which is constrained dynamically to move with the eddy). Finally, the classical permanent-form solutions obey a nonlinear dispersion relation, and possess a special, limited class of radial structures. These structures do not compare well with laboratory solitary eddy profiles (Sutyrin 1985); indeed, subsequent laboratory and numerical modelling (Sutyrin & Yushina 1988; Nezlin & Sutyrin 1989) have suggested the existence of a broader class of permanent-form eddies. Recently, Nycander & Sutyrin (1991) argued the surprising result that finite-amplitude reduced-gravity eddies of permanent form can assume effectively arbitrary radial profiles, provided that they also contain a weak imbedded dipole of the appropriate shape. The effects of an active lower layer on such solutions or the necessity of a finite amplitude to offset the effects of meridional dispersion, however, have not been previously considered.

The above questions form the main motivations for the present work. We examine the dynamics of radially symmetric eddies in two-layer models and suggest two basic results. (i) We argue that the class of permanent-form eddies may be generalized to include two active layers and that finite eddy amplitudes at scales larger than the deformation radius are not necessary to avoid meridional dispersion. Permanent-form eddies with arbitrary radial profiles and weak imbedded dipoles are found. The balance maintaining the eddy, namely steepening versus dispersion, remains of fundamental importance, with the dipole locally affecting eddy structure and propagation. The primary response of the lower layer is to develop a counter-rotating flow, consistent with a vanishing barotropic transport. (ii) A second result concerns

the effects of flows in the lower layer on eddy dynamics. These occur both in response to the upper-layer eddy, and as a result of the internal dynamics of the lower layer. Such flows influence eddy structure and propagation provided the lower layer has a non-trivial dynamical identity. The latter term (i.e. 'non-trivial identity') is defined in terms of a non-analytic potential-vorticity function in the lower layer. These, in turn, imply that fluid trapped in the lower layer possesses unique potential vorticity relative to the (passive) far-field potential vorticity. This potential-vorticity anomaly affects the eddy propagation rate due to the beta forces acting on the lower layer flow.

Our solutions suggest that the ability of rings and vortices to trap and transport fluid outside the main bowl of the eddy may be greater than previously imagined. Finally, we speculate that the existence of such permanent-form anticyclones may be related to the observed dominance of anticyclones, at least in the observations of SCVs, in the world's oceans.

Our model is introduced in §2 and our choices for scales are discussed. Various timescales of dynamic relevance are also identified. A perturbation expansion exploiting the differences in the various scales is carried out in §3. The role of asymmetries and of multi-valued potential-vorticity functionals is explored in §4 and the paper ends with a discussion.

2. Model development

Consider a two-layer, flat-bottom, inviscid, hydrostatic, Boussinesq ocean (see figure 1). The undisturbed upper layer is of thickness H_1 and the undisturbed lower layer is of thickness $H-H_1$. The density defect between the two layers is measured by the reduced-gravity parameter, g', and the beta-plane approximation is used. The quantities $\boldsymbol{u}$ and $\boldsymbol{v}$ denote upper and lower layer velocity, respectively. The quantities x and y denote east and north positions and t denotes time. The free surface is denoted η and h measures the deviation of the interface from its far-field depth. Under these conditions, the dimensional momentum and continuity equations describing the system are

$$\boldsymbol{u}_t+\boldsymbol{u}\cdot\nabla\boldsymbol{u}+(f_0+\beta_{\rm d}\,y)\,\boldsymbol{k}\times\boldsymbol{u}=-g\nabla\eta, \tag{1a}$$

$$h_t+\nabla\cdot(\boldsymbol{u}(H_1+h))=0, \tag{1b}$$

$$\boldsymbol{v}_t+\boldsymbol{v}\cdot\nabla\boldsymbol{v}+(f_0+\beta_{\rm d}\,y)\,\boldsymbol{k}\times\boldsymbol{v}=-g\nabla\eta+g'\nabla h, \tag{1c}$$

$$-h_t+\nabla\cdot(\boldsymbol{v}(H-H_1-h))=0, \tag{1d}$$

where the Coriolis parameter has been written $f_0+\beta_{\rm d}\,y$, the dimensional meridional gradient of f is $\beta_{\rm d}$, and a subscript x, y or t denotes a derivative. The symbol ∇ denotes the usual gradient operator and $\boldsymbol{k}$ is a vertical unit vector. (Note that the effects of the free surface η have been neglected in the continuity equations; see below.)

2.1. *Scales*

We are considering the evolution of depressions and elevations of the thermocline interface at $z=-H_1-h$; thus, we bring to the non-dimensionalization of (1) measures of the lengthscale, L, and the amplitude, δh, of the thermocline disturbance. Other externally set system parameters are the far-field upper-layer thickness and total fluid depth, H_1 and H, and the quantities g, g', f_0 and $\beta_{\rm d}$. These may be combined to yield two important intrinsic lengthscales, the beta scale, $L_\beta=f_0/\beta$ and the deformation radius, $R_{\rm d}=(g'H_1)^{\frac{1}{2}}/f_0$. Using typical parameters, these lengthscales

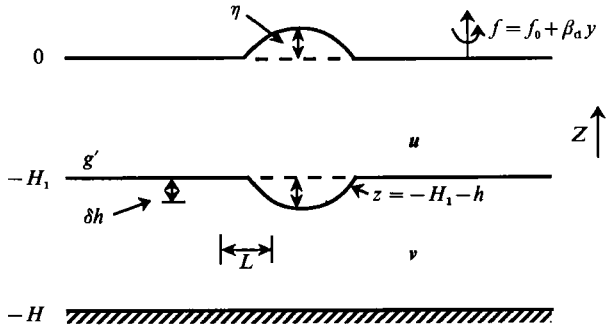

FIGURE 1. Model schematic. The upper layer has an undisturbed depth H_1 and the interface occurs at $z = -H_1 - h$. The free surface is denoted by η and the total fluid depth is H. The beta plane approximation is used. The Coriolis parameter f is written as $f = f_0 + \beta_d y$, where β_d is the north–south gradient of f.

are $L_\beta = 3000$ km and $R_d = 30$ km. A scale estimate for the free surface η is given by the hydrostatic balance to be

$$\eta \sim (g'/g)\,\delta h. \tag{2a}$$

We are motivated in our choice of scales by the oceanic situation where, for example, Gulf Stream rings are described by lengthscales of O(70–100 km) ($\gg R_d$) and timescales are long compared to f_0^{-1}. Thus, we expect velocities to be dominantly geostrophic in nature, and hence the upper-layer velocities to scale according to

$$U \sim \frac{g'\delta h}{f_0 L} = \frac{f_0 R_d^2\,\delta h}{L H_1}. \tag{2b}$$

An additional factor representing the ratio of the layer thicknesses is introduced for the lower-layer velocity scale:

$$V \sim O\left(\frac{H_1}{H} U\right). \tag{2c}$$

This reflects that the eddy is principally baroclinic and that (for the most part) the lower layer is simply responding to the upper-layer eddy.

Eddy propagation is driven by β, hence time will be scaled by $L/(\beta_d R_d^2)$, which represents the time taken for a non-dispersive planetary wave to propagate one characteristic lengthscale. In spite of its linear origins, the relevance of this timescale to nonlinear eddies was first demonstrated by Nof (1981), and argued for the nonlinear problem more recently by Cushman-Roisin, Chassignet & Tang (1990). (More thorough scale analyses of the two-layer equations, with application to eddies, have recently been conducted by Chassignet & Cushman-Roisin (1991) and Cushman-Roisin *et al.* (1992). The interested reader is referred to those studies for additional justification of the present space and time scales, as well as a broader exploration of possible interesting scalings.)

With these scales, the non-dimensional forms of (1) are

$$\hat{\beta} S \boldsymbol{u}_t + S\hat{\alpha}(\boldsymbol{u}\cdot\nabla\boldsymbol{u}) + (1+\hat{\beta}y)\,\boldsymbol{k}\times\boldsymbol{u} = -\nabla\eta, \tag{3a}$$

$$\hat{\beta} h_t + \nabla\cdot\boldsymbol{u} + \hat{\alpha}\nabla\cdot(\boldsymbol{u}h) = 0, \tag{3b}$$

$$\hat{\delta}\hat{\beta} S \boldsymbol{v}_t + \hat{\delta}^2 S\hat{\alpha}(\boldsymbol{v}\cdot\nabla\boldsymbol{v}) + \hat{\delta}(1+\hat{\beta}y)\,\boldsymbol{k}\times\boldsymbol{v} = -\nabla(\eta - h), \tag{3c}$$

$$\hat{\beta} h_t + \hat{\alpha}\hat{\delta}(\nabla\cdot\boldsymbol{v}h) - (1-\hat{\delta})(\nabla\cdot\boldsymbol{v}) = 0, \tag{3d}$$

which identifies the relevant non-dimensional parameters

$$\hat{\beta} = L/L_\beta, \quad \hat{\alpha} = \delta h/H_1, \quad \hat{\delta} = H_1/H, \quad S = R_d^2/L^2.$$

There are obviously many different parameter regimes for study in this model. The particular part of parameter space we have chosen focuses on S as the dominant small parameter, and is described by

$$1 \gg S \sim \hat{\alpha} \gg \hat{\delta} \sim S^2 \gg \hat{\beta} \sim S^3.$$

Clearly, we are examining a very special sector of parameter space; however, before moving on to the solution of this system we will argue that this sector is of interest geophysically and that it offers some useful analytical advantages.

Crudely speaking, the above ordering describes reasonably large-amplitude eddies, which are weakly affected by the lower layer and β. Typical values for L, g', H_1 and H as obtained from ring data, are 70 km, 2.5 cm/s^2, 500 m and 5000 m, respectively, which leads to

$$S \sim 0.3, \quad \delta = 0.1, \quad \hat{\beta} \sim 0.02.$$

These values are in rough agreement with the above ordering. Some further algebra demonstrates that the model applies to thermocline variations of $O(150$ m). This value is characteristic of deeper isopycnals in rings, if a little small.

As mentioned earlier, our interests are also partly motivated by SCV observations. Although it is true that SCVs are generally smaller than the first baroclinic deformation radius (which is an integral measure of the stratification) their lengthscales do tend to be larger than the deformation radius associated with their density defect. This results in small local Burgers numbers for SCVs (McWilliams 1985) and is in agreement with our above assumption about the relative size of S. Of course, other aspects of our model are at odds with SCV structures. Most notably, we examine a surface eddy and two-layer stratification. SCVs are more properly described as subsurface interthermocline lenses, the modelling of which involves at least three layers. Also, lenses generally require δh and the lens thickness scale to be comparable; here, we examine relatively small thermocline displacements. Nonetheless, the present part of parameter space is amenable to analytical analysis, and we will speculate on the relevance of the present results to SCVs in the hope that the dynamics involved will transcend the limits necessary for their strict asymptotic validity.

The above parameter ordering also describes the relevant physics. For example, steepening driven by density advection on a beta plane is proportional to $\beta_d vh$, while dispersive relative vorticity generation is proportional to $(\nabla \times \boldsymbol{u})_t$. The scaling rule $\hat{\alpha} \sim S$ equates their importance, which may be seen upon non-dimensionalizing the above quantities. Hence, this parameter range can be expected to yield KdV-like dynamics, and thus long-lived structures.

We now consider the $\hat{\delta}$ scaling. A major difference between two-layer and reduced-gravity systems is that the former may exhibit baroclinic instability. This tendency is, of course, lengthscale dependent and it has been argued by Phillips (1954) that the division between baroclinically stable and unstable disturbances occurs at the lengthscale $L \sim [g'(H_1 H_2)^{\frac{1}{2}}/f_0^2]^{\frac{1}{2}}$, which should be recognized as the geometric mean of the Rossby deformation radii appropriate to each layer. The above scaling for $\hat{\delta}$ describes lengthscales of precisely this order, suggesting that the analysis resides on the boundary of baroclinically stable eddies.

A separate feature of our analysis is the dynamic presence of the lower layer as an effect on eddy propagation. Lower-layer dynamics are expressed by potential-vorticity conservation, and it will be argued later that the lowest-order non-constant form of lower-layer potential vorticity is (non-dimensionally) $q_0 = \hat{\alpha}\hat{\delta}h + \hat{\beta}y$. Second-

layer potential vorticity is thus set by eddy topography and β. For the lower layer to act like anything more than a wave guide requires $\hat{\alpha}\hat{\delta} \sim \hat{\beta}$, which describes the above $\hat{\beta}$ scaling.

The above scaling also defines our lengthscale L in terms of the intrinsic lengthscales of the system, L_β and R_d, as

$$L = (R_\mathrm{d}^6 L_\beta)^{\frac{1}{7}}. \tag{4}$$

Thus L is smaller than the so-called intermediate scale $L_\mathrm{I} = (R_\mathrm{d}^2 L_\beta)^{\frac{1}{3}}$ (Charney & Flierl 1981; Yamagata 1982), but larger than the deformation radius. It will be therefore possible to simultaneously retain geostrophy at lowest order, but avoid the latitudinal dispersion effects associated with β_d.

It is also worth explicitly mentioning the timescales relevant to this problem. The first is the previously mentioned baroclinic propagation timescale, which when evaluated is

$$t = \frac{L}{\beta_\mathrm{d} R_\mathrm{d}^2} = \frac{R_\mathrm{d}^6 L_\beta}{\beta_\mathrm{d} R_\mathrm{d}^2 L^6} = S^{-3} f_0^{-1} \approx 30 \text{ days}.$$

It will also be of dynamical interest to consider the evolution on timescales long compared to the baroclinic timescale. This will be done by means of a multiple scale analysis, where the long timescale, τ, is given by

$$\tau = S^{-1} \frac{L}{\beta_\mathrm{d} R_\mathrm{d}^2} \approx S^{-4} f_0^{-1} \approx 4 \text{ months}.$$

Gulf Stream warm core rings are observed to drift in the Slope Water for times of $O(6$ months), while cold core rings appear to survive in the Sargosso Sea for even longer periods of time. Thus, introducing the above long τ timescale becomes of considerable interest. It will also turn out that the effects of steepening will be felt on this scale.

We also mention for later use the very rapid barotropic timescale, $T_\mathrm{bt} = (\beta_\mathrm{d} L)^{-1} \approx$ 7 days. This is the timescale for the barotropic adjustment of our two-layer system, and can be expected to be of importance in general initial-value problems. The analysis to follow can be performed with the explicit inclusion of motions on this timescale; however, we have here suppressed its appearance for simplicity. We nonetheless mention at appropriate points in the text the influence of rapid barotropic motions on the solution. There are, of course, other longer timescales which could potentially apply to the problem of ring evolution and which pertain to physics aside from that described here (e.g. latitudinal dispersion). We have here chosen to focus only on the two indicated timescales, and to neglect any slower evolution. (In a similar vein, we have also demonstrated to our own satisfaction that including a free surface does not alter the present results, provided the ratio $g'/g \ll S^3$. This constraint is easily met for typical oceanic reduced-gravity values, and we proceed using a rigid lid for the sake of simplicity.)

3. Expansion in S

A standard way of studying problems which involve evolution on more than one timescale is the method of multiple scales (Bender & Orszag 1978). A multi-scale analysis proceeds by considering all dependent variables as functions of both the fast and slow times, i.e. $q = q(t, \tau)$ and replacing time derivatives according to

$$\frac{\partial}{\partial t} \rightarrow \frac{\partial}{\partial t} + S \frac{\partial}{\partial \tau}.$$

The quantities t and τ are now considered as independent variables, and all dependent variables are expanded in powers of S. For convenience, the other non-dimensional parameters are written as

$$\hat{\alpha} = S\alpha, \quad \hat{\delta} = S^2\delta, \quad \hat{\beta} = S^3\beta,$$

where α, δ and β are all $O(1)$ constants.

The first two orders in the expansion reveal that the upper-layer flow is simply geostrophic and non-divergent, e.g.

$$\boldsymbol{k}\times\boldsymbol{u}_0 = -\nabla\eta_0, \qquad \nabla\cdot\boldsymbol{u}_0 = 0, \tag{5a, b}$$

where the subscript 0 denotes the order of the variable in the S expansion. Similar equations apply to the $O(S)$ velocities, i.e. $\boldsymbol{u}_1$, and the lower layer is found to be compensated (e.g. $\eta_0 = h_0$) through the first two orders. At this point, we also assert our interest in radially symmetric eddies by searching for solutions where $\eta_0 = \eta_0(r)$ (r denotes the radial coordinate in a cylindrical system attached to the eddy).

At $O(S^2)$, the upper-layer momentum equations yield

$$\alpha(\boldsymbol{u}_0\cdot\nabla u_0) + \boldsymbol{k}\times\boldsymbol{u}_2 = -\nabla\eta_2 \tag{6a}$$

from which it can be shown that

$$\nabla\cdot\boldsymbol{u}_2 = 0 \tag{6b}$$

for a radially symmetric η_0. The lower-layer momentum equations are simply geostrophic and non-divergent at this and the next two orders (i.e. from $O(S^2)$ to $O(S^4)$). Evolution on the baroclinic timescale, t, appears in the third order of the expansion. The upper-layer equations at $O(S^3)$ yields

$$\alpha(\boldsymbol{u}_0\cdot\nabla\boldsymbol{u}_1 + \boldsymbol{u}_1\cdot\nabla\boldsymbol{u}_0) + \boldsymbol{k}\times\boldsymbol{u}_3 + \beta y\boldsymbol{k}\times\boldsymbol{u}_0 = -\nabla\eta_3, \tag{7a}$$

$$\beta h_{0t} + \nabla\cdot\boldsymbol{u}_3 + \alpha(\boldsymbol{u}_2\cdot\nabla h_0 + \boldsymbol{u}_0\cdot\nabla\boldsymbol{h}_2) = 0, \tag{7b}$$

where compensation at $O(S)$ has been explicitly recognized. The divergence of the $O(S^3)$ velocities can be calculated from (7a) and used in (7b). Substituting where appropriate with other lower-order results eventually yields

$$\beta\eta_{0t} - \alpha\mathrm{J}(\eta_0, \nabla^2\eta_1) - \alpha\mathrm{J}(\eta_1, \nabla^2\eta_0) - \beta\eta_{0x} + \alpha\mathrm{J}(\eta_2 - h_2, \eta_0) = 0, \tag{8}$$

where ∇^2 denotes the usual Laplacian operator, while the lower-layer continuity equation can be written as

$$\beta\eta_{0t} + \alpha\mathrm{J}(\eta_2 - h_2, \eta_0) = \nabla\cdot\boldsymbol{v}_3. \tag{9}$$

J in (8) and (9) denotes the usual Jacobian operator:

$$\mathrm{J}(A, B) = A_xB_y - A_yB_x.$$

The calculation of the right-hand side of (9) requires expansion of the lower-layer momentum equations to $O(S^5)$, which yields

$$\delta\boldsymbol{k}\times\boldsymbol{v}_3 + \delta\beta y\boldsymbol{k}\times\boldsymbol{v}_0 = -\nabla(\eta_5 - h_5). \tag{10}$$

The above are used in (9) and we search for solutions propagating at the constant rate c. Under these conditions, the solution to (9) can be written

$$\eta_2 - h_2 + \frac{c\beta}{\alpha}y = K(\alpha\delta\eta_0 + \beta y), \tag{11}$$

where K is an as yet unspecified function. We also mention that the retention of the

barotropic timescale, T_{bt}, here results in a linear, dispersive barotropic wave equation for lower-layer pressure $\eta_2 - h_2$. The solution in (11) represents the asymptotic limit (at large T_{bt}) of the general time-dependent solution.

Equation (11) is a somewhat surprising result and its content is worth examining. Recall that the second-layer lowest-order velocity is simply geostrophic and related to the $O(S^2)$ pressure. Thus the left-hand side of (11) is recognized as a formula for the lower-layer 'streak function', i.e. the stream function appropriate to a frame attached to the propagating eddy. Recall that particles move along contours of constant streak function. It is also the case that two-layer models of the sort studied here are subject to potential-vorticity conservation in both layers, where the exact dimensional definition of, say, lower-level potential vorticity is

$$q_2 = \frac{\nabla \times v + f}{h_2}. \tag{12}$$

Non-dimensionalizing and expanding (12) reveals that the lowest-order non-constant contribution to q_2 is $q_{20} = \alpha\delta\eta_0 + \beta y$, demonstrating that potential vorticity in the lower layer is governed by eddy topography and β. Equation (11) is therefore immediately recognized as the expression of potential-vorticity conservation in the lower layer.

There are thus two separate cases of interest; namely (i) the case with no closed q_{20} contours and (ii) the case where some q_{20} contours are closed. In both cases, the form of K on q_{20} contours extending to infinity is straightforward to determine, and is

$$K(Z) = (c/\alpha)\, Z. \tag{13}$$

Of course, inside a closed q_{20} contour, (13) is not required, and some other function may apply. Although the study of such non-analytic potential vorticity fields is interesting, we will not pursue them at this order. Rather, we will proceed assuming that (13) holds everywhere, including inside closed q_{20}. (The case of closed q_{20} contours and non-analytic potential vorticity will be of rather more interest on the longer timescale.) In this case, (11) may be evaluated and used in (8) to yield

$$-\beta(c+1)\,\eta_{0x} = \alpha(\mathrm{J}(\eta_0, \nabla^2\eta_1) + \mathrm{J}(\eta_1, \nabla^2\eta_0)) \tag{14}$$

which applies everywhere in the domain. Multiplying (14) by x and area integrating over the entire plane yields, after several partial integrations,

$$\beta(c+1)\iint \eta_0 \,\mathrm{d}A = 0, \tag{15}$$

an equation identical to one first found by Flierl (1984*b*) in an appendix on quasi-geostrophic eddies.

We are interested in monopoles, and will enforce that interest by requiring the area integral of η_0 to be non-zero. (Note, this constraint also underscores a fundamental difference between the present analysis and the 'modon plus rider' solutions discussed by Flierl *et al.* (1980). There, the symmetric rider met a 'no net angular momentum' constraint. That would only be possible here if the η_0 integral vanished.) Hence (15) requires $c = -1$, the interpretation of which is that at the lowest order the eddy structure drifts west at the long non-dispersive planetary phase-speed limit. This result is consistent with our scaling (in particular with (4)), which focuses on lengthscales larger than the deformation radius. (The above result for c also holds if K is non-analytic. A discussion is given in the Appendix.)

Clearly then, the only non-trivial solutions for η_1 must satisfy the homogeneous form of (14). Three obvious solutions are $\eta_1 = q(r)$ for any function q, $\eta_1 = \eta_{0r}\cos\theta$ and $\eta_1 = \eta_{0r}\sin\theta$. The first can be simply absorbed into η_0, and the others represent $O(S)$ displacements of η_0 in the zonal and meridional directions, respectively. A suitable choice of eddy centre eliminates the latter two. In view of the above, and given the almost passive nature of η_1, we will assume $\eta_1 \equiv 0$ for the remainder of this analysis.

Equation (11) also yields

$$\eta_2 - h_2 = -\delta\eta_0 \tag{16}$$

everywhere. This demonstrates that the lower layer rotates in the opposite sense to the upper layer, and in such a manner that the lowest-order barotropic transport vanishes, i.e. $\boldsymbol{u}_0 + \boldsymbol{v}_0 = 0$. (Recall that $\boldsymbol{k}\times\boldsymbol{v}_0 = -\nabla(\eta_2 - h_2)$.) The relative thicknesses of the two layers, with the lower-layer thicker, allows the weak deep flow to offset the upper-layer transport. We also mention that (16) automatically satisfies the no-net-angular-momentum theorem of Flierl *et al.* (1983) at this order.

The first appearance of the long τ timescale comes at $O(S^4)$ of the expansion. The upper-layer equations at this order are

$$\beta\boldsymbol{u}_{0t} + \alpha(\boldsymbol{u}_2\cdot\nabla\boldsymbol{u}_0 + \boldsymbol{u}_0\cdot\nabla\boldsymbol{u}_2) + \boldsymbol{k}\times\boldsymbol{u}_4 = -\nabla\eta_4, \tag{17a}$$

$$\beta\eta_{0\tau} + \nabla\cdot\boldsymbol{u}_4 + \alpha(\nabla\cdot(\boldsymbol{u}_3\eta_0) + \nabla\cdot(\boldsymbol{u}_0 h_3)) = 0, \tag{17b}$$

where the fact that η_1 vanishes has been used. The divergence of the fourth-order velocity field can be calculated from (17*a*). Substituting the result in (17*b*), along with the expressions for $\boldsymbol{u}_3$ from earlier results yields

$$\mu\beta\eta_{0x} - \alpha\mathrm{J}(\eta_3 - h_3, \eta_0) + \alpha\beta\eta_0\eta_{0x} + \beta\nabla^2\eta_{0x} = -\alpha(\mathrm{J}(\eta_2, \nabla^2\eta_0) + \mathrm{J}(\eta_0, \nabla^2\eta_2)). \tag{18}$$

The fact that $\eta_0 = \eta_0(r)$, and the restriction to stationary-state solutions, so that $\eta_{0\tau} = -\mu\eta_{0x}$, have been used to deduce (18). Clearly, additional information about lower-layer pressure, $\eta_3 - h_3$, is necessary to close the problem.

Lower-layer continuity at $O(S^4)$ leads to

$$-\mu\beta\eta_{0x} + \alpha\mathrm{J}(\eta_3 - h_3, \eta_0) = \nabla\cdot\boldsymbol{v}_4 \tag{19}$$

and examination of (3) demonstrates that the right-hand side can be evaluated from the $O(S^6)$ lower-layer momentum equations. The final form of (19) is then

$$-\mu\delta\beta\eta_{0x} + \alpha\delta\mathrm{J}(\eta_3 - h_3, \eta_0) - \delta\beta\nabla^2\eta_{0x} + \mathrm{J}(\eta_3 - h_3, \beta y) = 0, \tag{20a}$$

which, after some algebra, can be written as

$$\mathrm{J}\left(\eta_3 - h_3 + \frac{\mu\beta}{\alpha}y - \delta\nabla^2\eta_0, \alpha\delta\eta_0 + \beta y\right) = 0. \tag{20b}$$

It is somewhat tedious, but relatively straightforward, to demonstrate that (20*b*) is again related to q_2 conservation. It expresses, in effect, the relation between the next-order corrections to the lower-layer streak function, represented by $\eta_3 - h_3 + (\mu\beta/\alpha)y$, and the weak tendency to develop relative vorticity necessary to simultaneously conserve q_2 and obtain a steadily propagating eddy. It should also be noted that the quantity μ represents an $O(S)$ correction to the main eddy propagation rate, $c = -1$.

The solution to (20*b*) is clearly

$$\eta_3 - h_3 + \frac{\mu\beta}{\alpha}y - \delta\nabla^2\eta_0 = G(\alpha\delta\eta_0 + \beta y) = G(q_{20}), \tag{21}$$

where, by the usual far-field arguments, a formula analogous to (13) applies to any q_{20} contour connected to the far field. (It is also true here that retention of the barotropic timescale converts (20*b*) to a linear, dispersive wave equation, the solution of which tends asymptotically to (21).) The quantity $\eta_3 - h_3$ now being determined in general by (21), (18) becomes

$$\beta\left(\frac{\alpha\eta_0^2}{2}+\nabla^2\eta_0+\frac{G}{\delta}\right)_x = -\alpha[\mathrm{J}(\eta_2,\nabla^2\eta_0)+\mathrm{J}(\eta_0,\nabla^2\eta_2)]. \tag{22}$$

The right-hand side of (22) simplifies considerably because of the symmetry in η_0, and is proportional to (denoting the azimuthal coordinate of the eddy-centred radial system as θ):

$$\mathrm{L}(\eta_2) = \frac{\eta_{0r}}{r}\nabla^2\eta_{2\theta} - \frac{\eta_{2\theta}}{r}\left(\frac{1}{r}\frac{\partial}{\partial r}r\frac{\partial}{\partial r}\eta_0\right)_r. \tag{23}$$

Equation (23) can be viewed as defining a third-order, linear, non-constant coefficient operator acting on η_2, and as such, the operator L has the adjoint

$$\bar{\mathrm{L}}(v) = \frac{1}{r}(\nabla^2\eta_0)_r v_\theta - \frac{\eta_{0r}}{r^3}v_{\theta\theta\theta} - \left(r\left(\frac{\eta_{0r}}{r^2}v_\theta\right)_r\right)_r. \tag{24}$$

We have found three solutions to the homogeneous form of (24), namely

$$v^{(1)} = q(r) \text{ for any function } q, \quad v^{(2)} = r^2\sin\theta, \quad v^{(3)} = r^2\cos\theta. \tag{25}$$

Of these, $v^{(3)}$ can be used to place a constraint of considerable importance on eddy structure. (The other two add no constraints due to the symmetry of η_0.) Equation (22) becomes upon multiplication by $v^{(3)}$

$$-\frac{\beta r^2}{\alpha}(\alpha\eta_0\eta_{0r}+(\nabla^2\eta_0)_r+G'\alpha\eta_{0r})\cos^2\theta = \frac{\partial}{\partial\theta}(F_1)+\frac{\partial}{\partial r}(r\eta_{0r}\eta_{2r}\sin\theta - r\eta_{0rr}\eta_2\sin\theta), \tag{26a}$$

where

$$F_1 = r\cos\theta\eta_{0r}\nabla^2\eta_2 - r\cos\theta\eta_2(\nabla^2\eta_0)_r + \sin\theta\eta_{0r}\frac{\eta_{2\theta}}{r} - \cos\theta\frac{\eta_{0r}}{r}\eta_2. \tag{26b}$$

Integrating (26*a*) azimuthally from 0 to 2π thus yields

$$\beta\pi r^2(\alpha\eta_0\eta_{0r}+(\nabla^2\eta_0)_r)+\beta\alpha\eta_{0r}r^2\int_0^{2\pi}G'\cos^2\theta\,\mathrm{d}\theta = -\alpha\pi\frac{\partial}{\partial r}[r\eta_{0r}\eta_{2sr}-r\eta_{0rr}\eta_{2s}], \tag{27a}$$

where

$$\eta_{2s} = \frac{1}{\pi}\int_0^{2\pi}\eta_2\sin\theta\,\mathrm{d}\theta. \tag{27b}$$

The quantity η_{2s} obviously represents the radial structure of a dipole which is imbedded within the otherwise symmetric eddy. It is interesting that the η_{2s} structure may be obtained directly from (27*a*), namely

$$\eta_{2s} = -\eta_{0r}\int_\infty^r\left\{\frac{\beta}{\alpha z\eta_{0z}^2\pi}\int_\infty^z\left[p\alpha\pi\eta_{0p}+\pi p^2(\nabla^2\eta_0)_p+\alpha p^2\eta_{0p}\int_0^{2\pi}G'\cos^2\theta\,\mathrm{d}\theta\right]\mathrm{d}p\right\}\mathrm{d}z. \tag{27c}$$

The above is similar to (40) in Nycander & Sutyrin (1991) and, for a purely analytic potential-vorticity function G, can be obtained from that result in the limit of small disturbances. Equation (27*c*) leads naturally to a main conclusion of this paper; namely, that essentially arbitrary radial profiles $\eta_0(r)$ can be associated with

permanent-form eddies. It is, of course, required that such an eddy contain an asymmetry (in particular, a dipole) of the structure defined by (27*c*). However, since the dipole is weak ($O(S^2)$), it is likely that its presence would be undetected in oceanographic observations, and perhaps unnoticed in the laboratory. Such considerations are of concern when considering theory–laboratory comparisons like those discussed in Sutyrin (1985) and Nezlin & Sutyrin (1989). It also follows from (27*a*) that the lowest-order eddy structure is subject to the constraint

$$\int_0^\infty \left[\beta\pi r^2(\alpha\eta_0\,\eta_{0r}+(\nabla^2\eta_0)_r)+\beta r^2\eta_{0r}\,\alpha\int_0^{2\pi} G'\cos^2\theta\,\mathrm{d}\theta\right]\mathrm{d}r=0. \tag{28}$$

Examples of solutions to (27*a*) are the subject of the next section. First, however, we point out that (28) is the expression of the no-net-angular-momentum theorem to this order. To see this, note that (27*a*) may be written

$$\beta\int_0^{2\pi} x\left(\frac{\alpha\delta(\eta_0)^2}{2}+\eta_3-h_3\right)_x r\,\mathrm{d}\theta=-\alpha\delta\pi\frac{\partial}{\partial r}\{r\eta_{0r}\,\eta_{2sr}-r\eta_{0rr}\,\eta_{2s}\}. \tag{29}$$

An integration over r then yields

$$\beta\int\int\left(\frac{\alpha\delta(\eta_0)^2}{2}+\eta_3-h_3\right)\mathrm{d}A=0 \tag{30}$$

after one integration by parts. The integrand in (30) is seen to be the $O(S)$ contribution to the barotropic mass transport stream function, thus validating the above conjecture.

4. Almost radially symmetric eddy structure

The structure functions, $G(q_{20})$ (see (21)), fall into either the analytic or non-analytic category. We have studied both choices and examples appropriate to each will be discussed here. The simplest case is that of analytic G, in which the form of G is determined by the far field (see e.g. (13)), and assumed to hold everywhere (even within closed q_{20} contours, should they occur). Thus, in general,

$$G=\frac{\mu}{\alpha}(\alpha\delta\eta_0+\beta y) \tag{31}$$

and this can be used in (27*c*) to yield a formula for η_{2s}. In principle, one can evaluate (27*c*) numerically for a given $\eta_0(r)$ (subject to some weak far-field constraints on $\eta_0(r)$, see below) following a procedure like that used in Nycander & Sutyrin (1991). For the purpose here of illustrating the connection between given η_{2s} and η_0 profiles as simply as possible, however, we have chosen to construct the coupled (η_{2s},η_0) pair in a different fashion. In effect, we will take the η_{2s} structure as given and calculate the associated $\eta_0(r)$. Such a procedure is simpler to manage numerically and yields a more immediate physical understanding of the dipole–monopole interaction. (This procedure is also essentially equivalent to evaluating (27*c*).) Therefore, for a given η_{2s} (27*a*) becomes

$$\eta_{0rrr}+\frac{1}{r}\eta_{0rr}+\frac{1}{r}\frac{1}{\beta r-\alpha\eta_{2s}}[\alpha r\eta_{2srr}+\alpha\eta_{2sr}-\beta+\beta r^2\mu+\beta\alpha r^2\eta_0]\,\eta_{0r}=0, \tag{32}$$

which for a given dipole, η_{2s}, is a non-constant-coefficient, nonlinear equation for η_0.

The boundary conditions on (32) are that the eddy be isolated, i.e. η_0 and all its derivatives vanish for large r, and at $r = 0$ it is required that η_0 be finite and that $\eta_{0r} = 0$. These conditions make (32) an eigenvalue problem for the parameter μ, while the nonlinearity of (32) will connect μ and the amplitude of η_0. It is also noted that at large r, (32) asymptotes to

$$\eta_{0rrr} + \frac{1}{r}\eta_{0rr} + \frac{1}{r^2}(\mu r^2 - 1)\eta_{0r} = 0, \tag{33}$$

where it has been implicitly assumed that η_0 and η_{2s} both decay in the far field. Decaying solutions thus require $\mu < 0$, demonstrating that this class of eddy meets the isolation constraint by exceeding the far-field planetary wave speed limit. The only possible far-field response is therefore evanescent. A second result from (33) is that

$$\eta_0 \approx K_0(|\mu|\, r) \quad \text{for} \quad r \to \infty, \tag{34}$$

where K_0 denotes the decaying modified Bessel function of order zero. (Note that this far-field structure meets the requirements necessary to obtain (33). Also, η_{2s} is seen to decay adequately in the far field (upon the substitution of (34) in (27*c*)) in order for (33) to apply.) It is also possible to analyse (32) in the limit of $r \to 0$. We require $\eta_{2s} = 0$ at $r = 0$, but only that η_{2sr} be finite (see (27*b*)). The result is

$$\eta_0 \sim r^2 \quad \text{as} \quad r \to 0. \tag{35}$$

Finally, evaluating (28) for this G eventually yields

$$\mu = -\frac{\frac{1}{2}\alpha \iint (\eta_0)^2 \, \mathrm{d}A}{\iint \eta_0 \, \mathrm{d}A}, \tag{36}$$

a formula related to one first noticed by Nof (1981) in the context of lens-like eddies and to one valid in a more general context by Cushman-Roisin (1986). Here the previously mentioned requirement of westward propagation also demonstrates the important result that only anticyclonic solitary eddies exist, i.e. $\iint \eta_0 \, \mathrm{d}A > 0$.

4.1. *Solutions*

Equation (32) represents a generalization of the classical class of planetary solitary waves. To see this, note that the special case of $\eta_{2s} = 0$ reduces (32) to

$$\frac{1}{r}\frac{\partial}{\partial r} r \frac{\partial}{\partial r}\eta_0 + \mu\eta_0 + \frac{\alpha}{2}(\eta_0)^2 = 0, \tag{37}$$

which is the equation studied previously by Flierl (1979) in the context of quasi-geostrophic eddies interacting with shear, and by Mikhailova & Shapiro (1980), Petviashvili (1980), Charney & Flierl (1981) and Petviashvili & Yan'kov (1982) for (effectively) the case of weakly nonlinear eddies at scales larger than the deformation radius.

For non-zero η_{2s}, the structure equation (32) is generally more complicated, but still represents a tractable numerical problem. We have solved (32) for the special case:

$$\eta_{2s} = a_0(r)(r-2)^3, \quad r < 2, \tag{38a}$$

$$\eta_{2s} = 0, \quad r \geqslant 2, \tag{38b}$$

for various values of a_0. The parameter μ was set to -1, and the asymptotic solution in (34) was used to generate a one-parameter family of estimates for η_0, η_{0r} and η_{0rr} at $r = 10$. The remaining parameters, α, δ and β, were all given values of 1. Equation (32) was then integrated to $r = 0$, and the quantity η_{0r} was checked. The one available parameter at $r = 10$ was then adjusted until $\eta_{0r}(0)$ vanished.

Solutions of (32) for various values of a_0 are shown in figure 2(*a*). Recalling (27*b*), it is seen that positive values for a_0 correspond to dipoles with low pressure to the north. Solutions for $a_0 = -0.1$, 0.1 and 1 are shown. Also shown for comparison is the classical solution of Flierl and Petviashvili & Yan'kov, which here corresponds to the choice $a_0 = 0$. Figure 2(*b*) contains the profiles of azimuthal velocity η_{0r} for each of the examples in figure 2(*a*).

The main tendency in these solutions is that negative a_0 values result in lower-amplitude eddies, and positive a_0 values result in higher-amplitude eddies. These results may be understood in terms of a simple interaction of the imbedded dipole and the radial eddy. A solitary dipole with a low pressure north of a high will develop an eastward propagation effect due to nonlinear centre–centre interaction. In contrast, a dipole consisting of a high pressure north of a low (i.e. negative a_0) develops a westward propagation tendency due to the same mechanism. (Such interactions are at the heart of modon propagation.) Equation (36) demonstrates that μ is ultimately a result of the global eddy structure; however, locally, the eddy can be modified considerably by the dipole. It is clear from (36) that larger amplitudes are associated with greater westward drifts. This mechanism is ultimately the source of the nonlinear steepening in our model. For negative a_0, the amplitude of the eddy near the eddy centre is relatively low (compared to $a_0 = 0$). The westward drift rate of this amplitude by itself is too slow to maintain the permanency in form. The necessary additional push comes from the advective effect of the dipole. These arguments are modified in the obvious way for a_0 positive.

4.2. *Anomalous potential vorticity*

We now explore the consequences on eddy structure and propagation of discontinuities in lower-layer potential vorticity. A first constraint on q_2 structure is that a G function of the form in (31) is required on any streaklines connected to the far field. The opportunity to introduce any other structure requires closed q_{20} contours. Assuming that this occurs, there are still at least two other constraints that the lower-layer q_2 should be required to meet; namely, continuity of lower-layer pressure and velocity on the bounding streakline. These constraints on the potential–vorticity functional inside closed q_{20}, can be expressed as

$$G(q_{20c}) = \frac{\mu}{\alpha} q_{20c} \quad \text{and} \quad \frac{\partial}{\partial q_{20}} G(q_{20c}) = \frac{\mu}{\alpha}, \tag{39a, b}$$

where q_{20c} denotes the critical bounding q_{20} contour.

Although (39) restricts the class of available functions, many still are acceptable. We will here proceed with the specific choice

$$G(q_{20}) = a_0(q_{20} - q_{20c})^2 + \frac{\mu}{\alpha} q_{20}. \tag{40}$$

Also, for the purposes of this discussion, we will simplify (27*a*) by assuming $\eta_{2s} \equiv 0$.

For radially symmetric η_0, the closed q_{20} streaklines are generally as depicted in

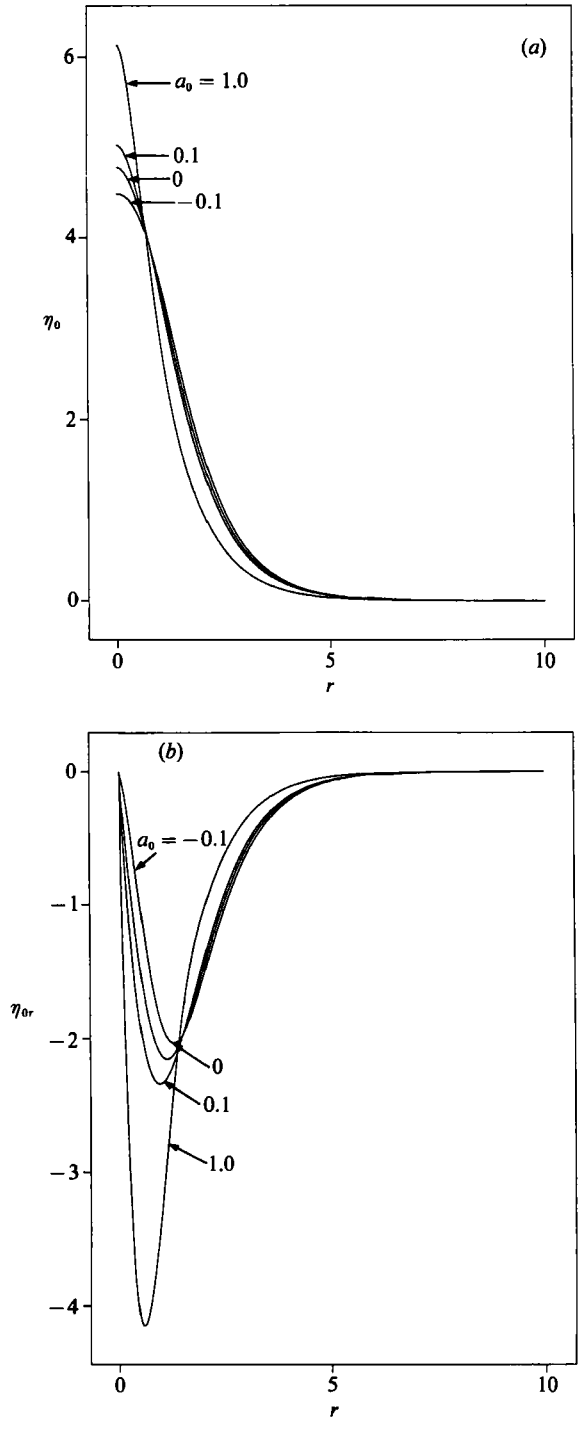

FIGURE 2. (*a*) Radial eddy amplitude and (*b*) azimuthal velocity against radial location r for several dipoles of differing strength. The values of a_0, measuring the strength of the imbedded dipole, are indicated and the eddy drift, μ, is always -1. Negative a_0 induces lower amplitudes in η_0. Structural permanency is maintained by dipole–monopole interaction.

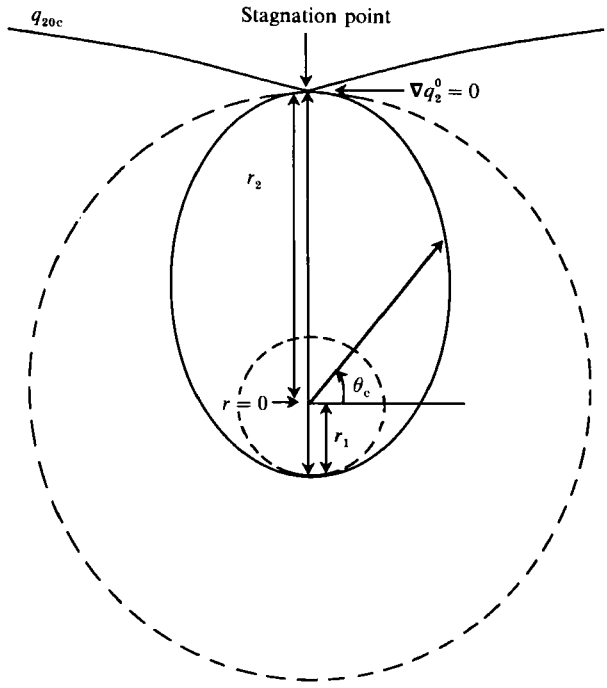

FIGURE 3. q_{20} schematic. Contours of constant $q_{20} = \alpha\delta\eta_0 + \beta y$ are displaced north relative to the radially symmetric eddy. The critical bounding contour q_{20c} is shown, as are the radii r_2 and r_1. The angle, θ_c, defining the boundary between interior and exterior potential vorticity for a given r is also indicated.

figure 3. The form of q_{20} requires east–west symmetry and, for an anticyclone, a lone stagnation point displaced to the north appears. The necessity of this structure can be demonstrated from the definition of q_{20}. Clearly, if closed q_{20} occurs, a local extremum in the structure of q_{20} exists on the bounding contour. Thus

$$\nabla q_{20} = \alpha\delta\nabla\eta_0 + \beta\hat{\jmath} = 0, \tag{41}$$

where $\hat{\jmath}$ is a unit vector in the north direction, which is a condition that can be met only on the north side of an anticyclone. Recalling (16), (41) is seen to describe the point where the lower-layer flow speed exactly matches the eddy drift rate.

It is also frequently the case that the eddy centre, defined by $\nabla\eta_0 = 0$, lies within the closed zone. Thus, our attention is drawn naturally to two critical radii, r_1 and r_2, where r_1 denotes smallest radial distance from the eddy centre to the bounding streakline, and r_2 denotes the distance from the eddy centre to the stagnation point (see figure 3). With (31) and (40), the structure function (27a) becomes

$$\eta_{0rrr} + \frac{1}{r}\eta_{0rr} - \frac{1}{r^2}\eta_{0r} + \mu\eta_{0r} + \alpha\eta_0\,\eta_{0r} = 0 \quad \text{for} \quad r > r_2, \tag{42a}$$

$$\eta_{0rrr} + \frac{1}{r}\eta_{0rr} - \frac{1}{r^2}\eta_{0r} + \frac{\alpha\eta_{0r}}{\pi}\left(\frac{\mu}{\alpha}\pi + \alpha a_0\,\delta\pi\eta_0 - 2a_0\,\alpha\delta\eta_0\,\theta_c - a_0\,\alpha\delta\eta_0\sin(2\theta_c) + \tfrac{4}{3}\beta a_0\, r\cos^3(\theta_c)\right.$$

$$\left. - q_{20c}\,a_0\,\pi + 2a_0\,q_{20c}\,\theta_c + a_0\,q_{20c}\sin(2\theta_c)\right) + \alpha\eta_0\,\eta_{0r} = 0 \quad \text{for} \quad r_1 < r < r_2 \tag{42b}$$

(where θ_c is defined by $\alpha\delta\eta_0(r)+\beta r\sin(\theta_c)=q_{20c}$), and

$$\eta_{0rrr}+\frac{1}{r}\eta_{0rr}-\frac{1}{r^2}\eta_{0r}+\alpha\eta_{0r}\left(2a_0\alpha\delta\eta_0+\frac{\mu}{\alpha}-2a_0\,q_{20c}\right)+\alpha\eta_0\,\eta_{0r}=0 \quad \text{for} \quad 0<r<r_1. \tag{42c}$$

Thus it is seen that the non-analytic functional complicates the nonlinearity of the structure function considerably, and this can be expected to affect the eddy propagation rate. Indeed, evaluating (28) yields

$$\mu=-\frac{\alpha\int\int_{-\infty}^{+\infty}\frac{\eta_0^2}{2}\,\mathrm{d}A+\frac{1}{\delta}\int\int_{\text{closed }q_{20}}\left[G-\frac{\mu}{\alpha}(q_{20})\right]\mathrm{d}A}{\int\int\eta_0\,\mathrm{d}A}, \tag{43}$$

which demonstrates that the deviation of the q_{20} structure from (31) inside q_{20} affects μ.

Although useful, (43) does not clearly display the mechanics determining the eddy drift rate. These are more clearly seen if the $O(S^3)$ upper-layer continuity equation (17*b*) is studied. Upon use of (7) to eliminate $\boldsymbol{u}_3$, (17*b*) reduces to

$$-\mu\beta\eta_{0x}+\nabla\cdot\boldsymbol{u}_4+\alpha\mathrm{J}(\eta_3-h_3,\eta_0)-\alpha\beta\eta_0\,\eta_{0x}=0. \tag{44}$$

Multiplying the above by x and area integrating yields

$$\underset{\text{(i)}}{\beta\mu\int\int_{-\infty}^{\infty}\eta_0\,\mathrm{d}A}+\underset{\text{(ii)}}{\alpha\int\int_{-\infty}^{\infty}\eta_0(\eta_3-h_3)_y\,\mathrm{d}A}+\underset{\text{(iii)}}{\alpha\beta\int\int_{-\infty}^{\infty}\frac{\eta_0^2}{2}\mathrm{d}A}=0. \tag{45}$$

(The vanishing of $\int\int_{-\infty}^{\infty}\boldsymbol{u}_4\cdot\boldsymbol{i}\,\mathrm{d}A$ (where $\boldsymbol{i}$ is a zonal vector), necessary to obtain (45) can be directly demonstrated from (17).) Equation (45) has the straightforward interpretation that, in general, the forces which must balance in a steadily propagating eddy are the (i) bulk Coriolis force due to the net eddy migration, (ii) pressure forces acting on the upper-layer eddy caused by lower-layer flows and (iii) the so-called beta force. Such a formula was also noticed by Flierl (1984*b*) where the pressure force was due to wave radiation rather than anomalous potential vorticity. He also found an induced southward motion caused by wave drag, which is absent here due to our search for permanent-form solutions. As such, (45) resembles (43). The exact equivalence of these equations can be demonstrated if (20*a*) is now multiplied by x and area integrated. The result is

$$\mu\delta\beta\int\int\eta_0\,\mathrm{d}A+\alpha\delta\int\int\eta_0(\eta^3-h^3)_y\,\mathrm{d}A-\beta\int\int_{-\infty}^{\infty}\eta_3-h_3\,\mathrm{d}A=0, \tag{46}$$

which relates net forces in the lower layer in a manner like that for (45). Clearly from (21)

$$\int\int_{-\infty}^{\infty}\eta_3-h_3\,\mathrm{d}A=\int\int_{-\infty}^{\infty}G\,\mathrm{d}A. \tag{47}$$

Substitution in (46) and recalling (31) demonstrates the conjecture.

It is interesting to note that if the lower-layer q_2 field is analytic, so that (31) applies everywhere, the pressure force contribution to (43) identically vanishes, and

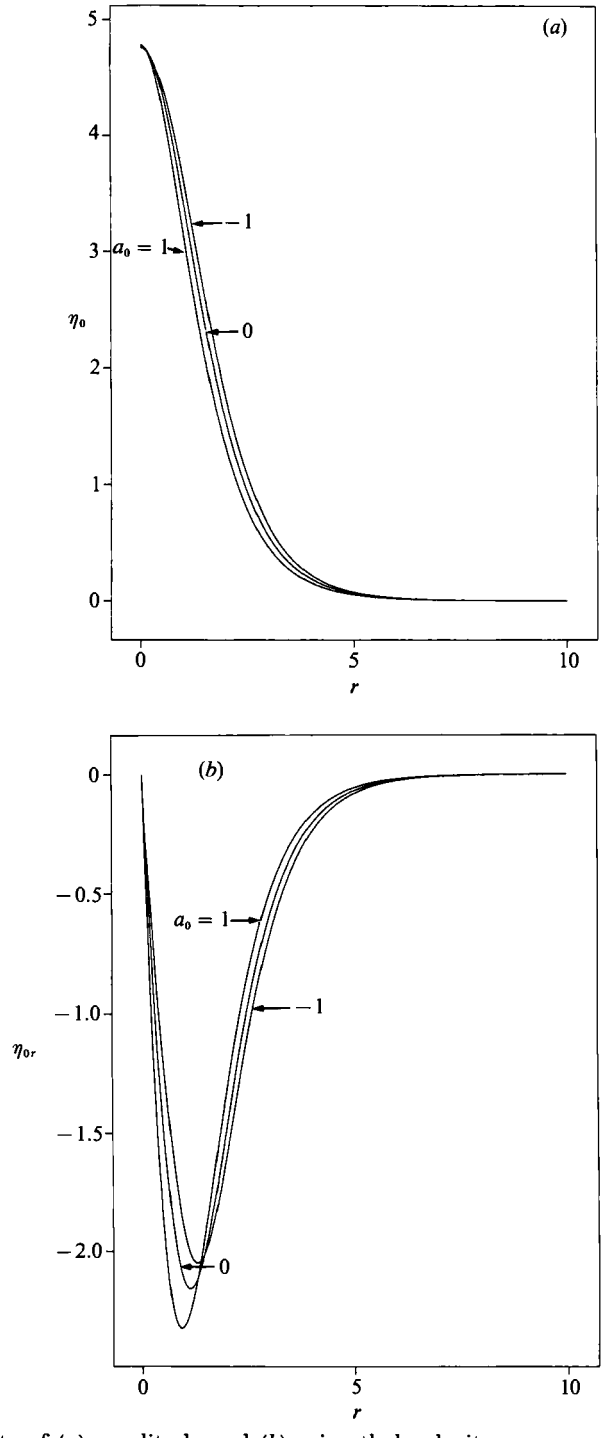

FIGURE 4. Plots of (*a*) amplitude and (*b*) azimuthal velocity versus radius for eddies with non-analytic lower-layer q. The values for a_0 are -1 and 1, and the curves are compared to the classical case given by $a_0 = 0$.

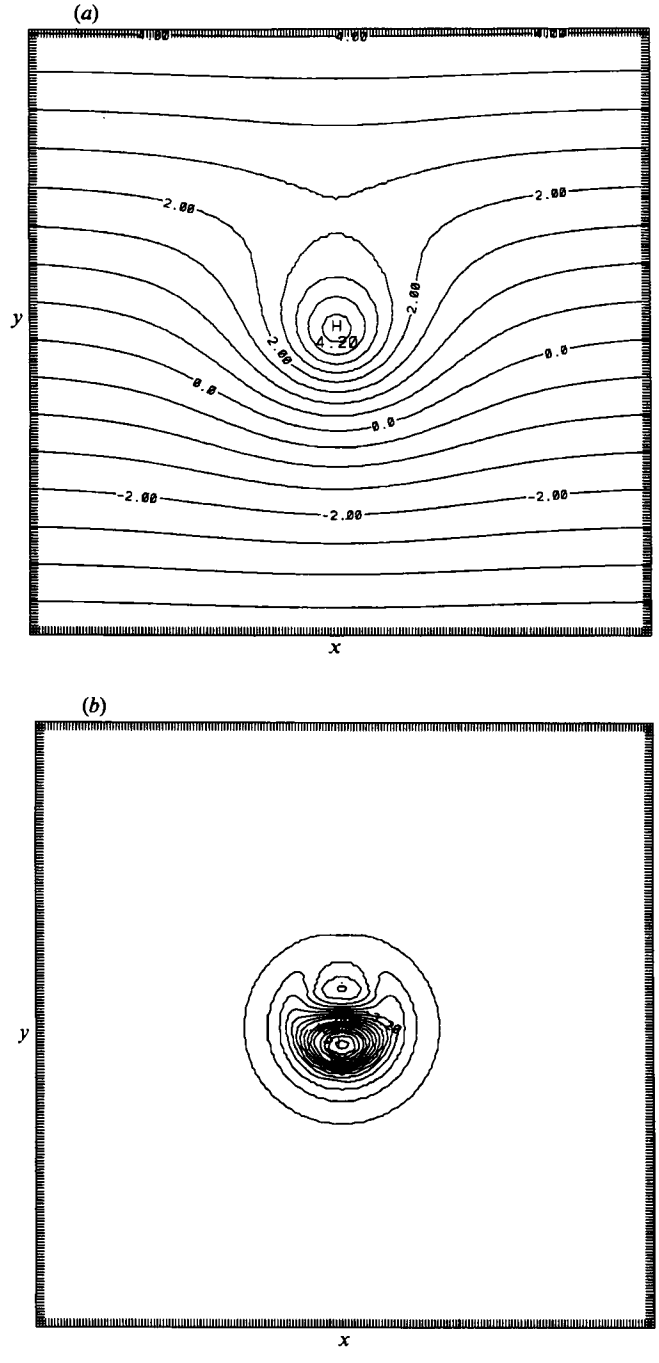

FIGURE 5. (*a*) Lowest-order potential vorticity and (*b*) lower-layer pressure, $\eta_3 - h_3$, for an isolated eddy with non-analytic q. $a_0 = 8$.

(36) results. The potential-vorticity functional in (31) is one which, in some sense, describes a passive lower-layer fluid. All deep motion is ultimately related to the eddy as a response to dispersion and drift. Equation (43) demonstrates that if this passive condition is not met, i.e. if the deep fluid has any non-trivial dynamic

identity (expressed by a unique potential vorticity), the propagation (and structure) of the eddy will be affected. Arguments can be made that ring generation events potentially involve a broad spectrum of lower-layer structures, from perfectly compensated initial conditions, to states with important deep flows. Perhaps (45) is related more to a general rule of eddy propagation rather than an exception.

We have solved (42) for several values of a_0; the results for η_0 for $a_0 = 1$ and -1 are shown in figure 4(*a*). The results for η_{0r} with the same a_0 values are shown in figure 4(*b*) and the classical results for $a_0 = 0$ are shown in both plots for comparison. For all solutions, the value of μ was set to -1, the values for α, δ and β were all set to 1, and (34) (still valid for large r) was used to generate a one-parameter family of solutions for η_0, η_{0r} and η_{0rr} at $r = 10$. Integration towards the origin was then begun according to (42*a*). When critical condition (41) was met, the governing equation was switched to (42*b*) and the critical value of q_{20c} was noted. Finally, the structure function was switched to (42*c*) when θ_c reached the value $-\frac{1}{2}\pi$. This procedure was repeated, and the single available parameter at $r = 10$ adjusted until $\eta_{0r}(0)$ vanished. Also, figure 5(*a*) shows a plot of $\alpha\delta\eta_0 + \beta y = q_{20}$, which contains closed q_{20} contours, and in figure 5(*b*) a plot of $\eta_3 - h_3$. For these plots, $a_0 = 8$.

To this point, we have only considered the dipolar corrections to the upper-layer structure. As the previous analysis shows, this part of the $O(S^2)$ field is connected dynamically to the lowest-order structure. On the other hand, a non-analytic potential-vorticity structure requires the presence of higher azimuthal modes at $O(S^2)$. This can be seen from (22), where it is noticed that the equation for the radial structure function of higher modes is inhomogeneous for non-analytic G. We have not explicitly calculated η_2, but can mention that analyses of the higher-order mode equations show vanishing solutions near $r = 0$ and decaying solutions for large r. Higher-order azimuthal corrections thus appear to be well behaved.

5. Discussion

The purpose of this study has been to examine long-lived eddies in stratified fluids of finite depth. Thus this work complements the existing theories of stationary eddies in reduced-gravity models, as well as Flierl's (1984*a*, *b*) seminal works on eddy radiation by drifting lenses. In particular, the present class of eddies is characterized by lengthscales of $O(70\text{ km})$, which corresponds to $S \ll 1$. Also, they reside on isopycnals which interact importantly with the lower layer; a typical dimensional value of far-field interface depth is roughly $O(500\text{ m})$ and the total fluid depth is 5000 m. These scales are all in reasonable agreement with observations of many warm eddies. Further, the present eddies differ dynamically from other eddy solutions involving dipoles (e.g. Flierl *et al.* 1980) in that the fundamental eddy structure is radially symmetric.

Accordingly, we have demonstrated that permanent-form, anticyclonic eddies can exist in stratified fluids with active lower layers and clarified the structure of the lower-layer flow in their vicinity. The basic response of the lower layer is to rotate cyclonically such that the net mass transport over both layers vanishes. This is essentially a result of Sverdrup dynamics, which come into play because of the lengthscale of the eddy. The lower-layer motion is forced by the eddy as it drifts at the non-dispersive planetary limit. Modifications to this drift are forced by the nonlinearity in the continuity equation. Deeper parts of an anticyclone move relatively fast and tend to overtake shallower parts. This steepening influence is balanced against the weak tendency for dispersion at these lengthscales. No motion

is excited in the far field as the perturbation to the drift speed is to the west; in effect, the eddies move too fast to generate waves in the (linear) exterior.

We have also found that effectively arbitrary radial structure can be associated with permanent-form two-layer eddies, provided that an appropriate, weak asymmetry exists within the eddy. The constraint on the otherwise arbitrary radial structure is that it decay according to a K_0 Bessel function rule. The asymmetries take the form of imbedded dipoles and these dipoles influence the eddy structure and propagation in a fairly simple fashion. For example, a dipole consisting of a high pressure over a low augments the westward drift of the eddies, sending lower-amplitude parts of an eddy to the west faster than would otherwise occur.

Further, the theory of permanent-form radial eddies can be extended to include a discontinuous potential-vorticity function in the lower layer. The effect of such flows on the upper-layer eddy structure and propagation are somewhat more complicated than for the case of imbedded dipoles; however, the relevant force balance is fairly straightforward. Anomalous lower-layer potential vorticity induces an asymmetric pressure distribution on the upper-layer eddy. The force balance of the Taylor column system thus involves this pressure force in addition to the usual beta and drift forces.

Both effects, i.e. upper-layer dipoles and lower-layer anomalous potential vorticity, can be simultaneously present in an eddy, demonstrating that the tendency for eddies to behave as long-lived structures is indeed profound. The generalization of this category of stationary solutions to include such diverse types of eddy structures and dynamics is perhaps the most surprising result of our analysis.

A natural question concerns how the present study applies to the real ocean. To this end, the above-mentioned result is a useful dynamical statement, given the apparent dominance of monopoles in the ocean. This analysis may provide a partial explanation for the observed bias of SCVs towards oceanic anticyclones. (It is also tempting to think that the present dynamics participate in Gulf Stream warm-ring evolution. On the other hand, it is observed that cold rings are also relatively long lived, and the present model clearly cannot be said to apply to them.) Further, the fact that arbitrary profiles can be associated with permanent-form eddies is important when comparing oceanic or laboratory eddies to theory. Finally, we conclude that eddy propagation rates and structure can be affected importantly by fluid dynamically trapped under the eddy, provided the trapped fluid has some non-trivial dynamic identity. Considering for a moment the circumstances resulting in the formation of warm rings, it is plausible that the potential-vorticity structure of a new ring spans the range of possibilities from fully compensated lower-layer flows to strong lower-layer flows of nearly arbitrary structure. Our latter result argues for the necessity of considering deep flows when predicting ring behaviour.

As a related implication, we have demonstrated that the circumstances in which deep fluid is dynamically trapped by the eddy are easily met. Estimates of eddy mass transport have previously focused on the fluid within the eddy baroclinic signature. Our analysis suggests such estimates might be in need of revision.

The significant question of the stability of our proposed solutions has not been addressed, but is of interest. Numerical experimentation (Swenson 1987) suggests that the modon plus rider solutions of Flierl *et al.* (1989) are unstable, a result which Swenson argues draws attention to non-quasi-geostrophic effects in nonliear eddies. It has further been argued that the trajectory of westward-propagating dipoles is unstable, owing to an intensification of one of the two pressure centres induced by trajectory perturbations (Makino, Kamimura & Taniuti 1981). With respect to the

former issue, the non-quasi-geostrophic effect of finite-amplitude thickness perturbations is central to our solutions. This fact, coupled with the weak nature of the imbedded dipole, complicates comparisons with Swenson's experiments. Further numerical experiments will provide the most direct route to addressing the fundamental stability of the present solutions. With regard to the latter issue, we note that the imbedded dipole present in our solutions need not obtain the classic dipole structure of high pressure north of low pressure. Thus, the unstable feedback between trajectory perturbations and the evolution of pressure centres need not occur. Hence, we speculate that our solutions may be less susceptible to trajectory instability than westward-propagating modons.

From a structural point of view, perhaps the aspect of our theory most likely to be field tested is the prediction of deep cyclonic flow underneath eddies. Observationally, little data are available to either refute or support this idea. On the other hand, some relevant observations were obtained during the study of warm core ring 82-B. Joyce & McDougall (1991) reported acoustic current measurements combined with standard hydrographic measurements to give maps of absolute azimuthal velocity for 82-B in April and June 1982. Both data sets indicate cyclonic flow underneath the eddy; the June velocities were observed to be in excess of 10 cm/s. To be fair, however, the statistical significance of the April cyclonic flow is questionable, and Joyce & McDougall (1991) state that the dynamic connection of the June deep cyclonic flow to 82-B cannot be clearly demonstrated. We nonetheless mention these data, as they are at least consistent with our analysis.

Numerical eddy models perhaps currently provide a more substantive test bed for our calculations, and to this end, the eddy studies of Chassignet & Cushman-Roisin (1991) support our finding of a counter-rotating deep flow under evolving eddies. It is also by now fairly well established numerically that anticyclones are considerably more stable than cyclones. Again, these tendencies are in agreement with our results.

Finally, we remark again on the effect of trapped deep fluid on eddy propagation. The existence of closed q_{20} contours occurs quite naturally for the scales which describe rings, i.e. the quantity $\alpha\delta\eta_0+\beta y$ generally develops isolated regions. The sensitivity of the eddy drift rate in (45) to the potential vorticity of the deep fluid suggests that the classical eddy propagation rate formulae, when applied to oceanic eddies, may be missing an important effect.

This research was sponsored by ONR contract N00014-89-J-1577 and NSF grant OCE-9012114. The authors particularly wish to recognize Ms S. Heseltine for her careful preparation of the manuscript and figures. This work was begun during a visit by G.G.S. to the Florida State University and continued during a visit by W.K.D. to the Shirshov Institute. Both authors gratefully acknowledge the hospitality of the host institutions during these trips.

Appendix

The purpose of this appendix is to demonstrate that the result of (15) that $c=-1$ holds even if K is non-analytic. To see this, note that the structure of the right-hand side of (14) is identical to that of (22). Therefore, $v^{(3)}$ of (25) can be used to modify (14) in a manner analogous to that which leads to (27a). The result is

$$\frac{\partial}{\partial r}\frac{\eta_{1s}}{\eta_{0r}}=\frac{-\beta(c+1)}{\alpha}\frac{1}{r(\eta_{0r})^2}\int_r^\infty r^2\eta_{0r}\,\mathrm{d}r, \tag{A 1}$$

where (13) has been used

$$\eta_{1s} = \int_0^{2\pi} \eta_1 \sin\theta \, \mathrm{d}\theta,$$

and it has been assumed that all dynamic quantities vanish as $r \to \infty$. Note that (13) applies for r outside any closed q_{20}, so (A 1) is completely general for large r. The presence of $(\eta_{0r})^2$ in the denominator of (A 1), however, is sufficient to ensure that

$$\frac{\partial}{\partial r}\frac{\eta_{1s}}{\eta_{0r}} \to \infty \quad \text{as} \quad r \to \infty,$$

unless $c = -1$. The above is disallowed as the perturbation scheme requires $\eta^1 \leqslant O(\eta^0)$ for all r. Thus, the result $c = -1$ is seen to depend only on the far field.

REFERENCES

Bender, C. & Orszag, S. 1978 *Advanced Mathematics Methods for Scientists and Engineers.* McGraw-Hill, pp. 593.

Berestov, A. L. 1981 Some new solutions for the Rossby solitons. *Izv. Acad. Sci. USSR Atmos. Oceanic Phys.* **17**, 60–64.

Charney, J. C. & Flierl, G. R. 1981 Oceanic analogues of large scale atmospheric motions. In *Evolution of Physical Oceanography* (ed. B. A. Warren & C. Wunsch), pp. 504–548. MIT Press.

Chassignet, E. & Cushman-Roisin, B. 1991 On the influence of the lower layer on an upper layer isolated ocean ring in a two-layer system. *J. Phys. Oceanogr.* **21**, 939–957.

Cushman-Roisin, B. 1986 Frontal geostrophic dynamics. *J. Phys. Oceanogr.* **16**, 132–143.

Cushman-Roisin, B., Chassignet, E. & Tang, B. 1990 Westward motion of mesoscale eddies. *J. Phys. Oceanogr.* **20**, 758–768.

Cushman-Roisin, B., Sutyrin, G. G. & Tang, B. 1992 Two-layer geostrophic dynamics. Part I: Governing equations. *J. Phys. Oceanogr.* (in press).

Ebbesmeyer, C., Taft, B. A., McWilliams, J. C., Shen, C. Y., Riser, S. C., Rossby, H. T., Biscayne, P. E. & Ostlund, H. G. 1986 Detection, structure and origin of extreme anomalies in a western Atlantic oceanographic section. *J. Phys. Oceanogr.* **16**, 591–612.

Flierl, G. 1979 Baroclinic solitary waves with radial symmetry. *Dyn. Atmos. Oceans* **3**, 15–38.

Flierl, G. 1984*a* Model of the structure and motion of a warm-core ring. *Austral. J. Mar. Freshwat. Res.* **35**, 9–23.

Flierl, G. 1984*b* Rossby wave radiation from a strongly nonlinear warm eddy. *J. Phys. Oceanogr.* **14**, 47–58.

Flierl, G. 1987 Isolated eddy models in geophysics. *Ann. Rev. Fluid Mech.* **19**, 493–530.

Flierl, G., Larichev, V. D., McWilliams, J. C. & Reznick, G. M. 1980 The dynamics of baroclinic and barotropic solitary eddies. *Dyn. Atmos. Oceans* **5**, 1–41.

Flierl, G., Stern, M. & Whitehead, J. A. 1983 The physical significance of modons: laboratory experiments and general integral constraints. *Dyn. Atmos. Oceans* **7**, 233–263.

Joyce, T. M. & McDougall, T. J. 1991 Physical structure and temporal evolution of Gulf Stream warm-core ring 82B. *Deep-Sea Res.* (in press).

Larichev, V. D. & Reznik, G. M. 1976 Two-dimensional Rossby soliton: an exact solution. *Rep. USSR Acad. Sci.* **231**, 1077–1079.

Makino, M., Kamimura, T. & Taniuti, T. 1981 Dynamics of two-dimensional solitary vortices in a low-β plasma with convective mode. *J. Phys. Soc. Japan* **50**, 980–989.

Malanotte-Rizzoli, P. 1982 Planetary solitary waves in geophysical flows. *Adv. Geophys.* **24**, 147–224.

Matsuura, T. & Yamagata, T. 1982 On the evolution of nonlinear planetary eddies larger than the radius of deformation. *J. Phys. Oceanogr.* **12**, 440–456.

McWilliams, J. C. 1984 The emergence of isolated, coherent vortices in turbulent flow. *J. Fluid Mech.* **146**, 21–43.

McWilliams, J. C. 1985 Submesoscale, coherent vortices in the ocean. *Rev. Geophys.* **23**, 165–182.

McWilliams, J. C., Gent, P. R. & Norton, N. J. 1986 The evolution of balanced, low-mode vortices on the β-plane. *J. Phys. Oceanogr.* **16**, 838–855.

Mikhailova, E. I. & Shapiro, N. B. 1980 Two-dimensional model of synoptic disturbances evolution in the ocean. *Izv. Akad. Nauk SSSR. Fiz. Atmos. Okeana* **16**, 823–833.

Nezlin, M. V. & Sutyrin, G. G. 1989 Long-lived solitary anticyclones in the planetary atmospheres and oceans, in laboratory experiments and in theory. In *Mesoscale/Synoptic Coherent Structures in Geophysical Turbulence* (ed. J. C. J. Nihoul & B. M. Jamart), pp. 701–720. Elsevier.

Nof, D. 1981 On the β-induced movement of isolated baroclinic eddies. *J. Phys. Oceanogr.* **11**, 1662–1672.

Nycander, J. & Sutyrin, G. G. 1991 Stationary translating anticyclones on the beta-plane. *Dyn. Atmos. Ocean.* (in press).

Petviashvili, V. I. 1980 Red spot of Jupiter and the drift soliton in a plasma. *JETP Lett.* **32**, 632–635.

Petviashvili, V. I. & Yan'kov, V. V. 1982 Two-layer vortices in a rotating stratified fluid. *Dokl. Akad. Nauk SSSR* **267**, 825–828.

Phillips, N. A. 1954 Energy transformations and meridional circulations associated with simple baroclinic waves in a two-level, quasi-geostrophic model. *Tellus* **6**, 273–286.

Stern, M. E. 1975 Minimal properties of planetary eddies. *J. Mar. Res.* **33**, 1–13.

Sutyrin, G. G. 1985 On the theory of solitary anticyclones in a rotating fluid. *Dokl. Akad. Nauk SSSR* **280**, 1101–1105 (Transl: *Earth Sci.* pp. 38–41).

Sutyrin, G. G. & Yushina, I. G. 1986 On the evolution of isolated eddies in a rotating fluid. *Izv. Akad. Nauk SSSR. Mekh. Zhid. i Gaza* **4**, 52–59 (Transl: *Fluid Dyn.* pp. 550–556).

Sutyrin, G. G. & Yushina, I. G. 1988 Formation of a vortical soliton. *Dokl. Akad. Nauk SSSR* **299**, 580–584 (Transl: *Sov. Phys. Dokl.* **33**(3), 179–181).

Swenson, M. 1987 Instability of equivalent barotropic riders. *J. Phys. Oceanogr.* **17**, 492–506.

Tang, B. & Cushman-Roisin, B. 1992 Two-layer geostrophic dynamics. Part II: Geostrophic turbulence. *J. Phys. Oceanogr.* (in press).

Yamagata, T. 1982 On nonlinear planetary waves: a class of solutions missed by the quasigeostrophic approximation. *J. Oceanogr. Soc. Japan* **38**, 236–244.